UNIVERSIDAD DE SEVILLA

Grado en Física

Trabajo fin de grado

PLASMA PHYSICS AND FUSION ENERGY

Enrique Hernández Lorenzo

Tutor:

José Cotrino Bautista

Departamento de Física Atómica, Molecular y Nuclear

PLASMA PHYSICS AND FUSION ENERGY

Enrique Hernández Lorenzo

Sevilla, 27 de Junio de 2017

List of notations

Notation	Meaning
JET	Joint European Torus
ITER	International Thermonuclear Experimental Reactor
TFTR	Tokamak Fusion Test Reactor
ICF	Inertial Confinement Fusion
MCF	Magnetic Confinement Fusion
RFP	Reversed Field Pinch
MHD	Magnetohydrodynamics
NSTX	National Spherical Torus Experiment

List of symbols

Symbol	Meaning
R_0	Major radius
a	Minor radius
Q	Gain factor
Δ^*	Elliptic laplacian
Ψ	(Magnetic) flux function
ψ	(Magnetic) flux function- dimensionless
β	Normalized plasma pressure
ε	Inverse aspect ratio
κ	Elongation
δ	Triangularity
q_*	Kink safety factor
Δ	Shafranov shift

Index

1. Abstract

A review on the equilibrium problem in magnetic confinement fusion plasmas is presented here. We first introduce the motivations to keep researching in fusion plasma physics, and the current state of actual fusion experiments. Afterwards, we briefly discuss the magnetohydrodinamics (MHD) equilibrium model and the resulting Grad-Shafranov equation. The equilibrium problem is solved by means of a MATLAB code that constructs approximated analytical solutions for a variety of geometries and conditions consistent with actual fusion experiments. The solution provides some physical quantities of interest that we analyze. Then, the equilibrium is also found for Taylor states with another MATLAB code, and a not so deep analysis is done.

2. Objectives and methodology

The main objective of this work is to gain an overall, qualitative understanding on the magnetic confinement fusion (MCF) problem, and specifically to be able to make detailed, quantitative theoretical calculations associated with the equilibrium problem. Of course, this requires first to obtain a basic understanding of plasma physics and MHD theory. This was done in the first stage of the work, although it is not treated in detailed here (except for MHD equilibrium, which is studied in section 4).

Second, in order to give a review of the overall situation of MCF energy research, the basics of the design and properties of different fusion confinement devices as well as a qualitative understanding of the transport and stability problem, specially focused to the difficulties arising in actual tokamaks experiments, was developed. This is mostly addressed in section 3.

Finally, as an application of this knowledge, a couple of codes built in MATLAB were used to obtain quantitative results on the equilibrium problem, for different sets of geometrical and physical conditions. These codes are able to solve systems of nonlinear, coupled algebraic equations, which ultimately determine the coefficients of the proposed analytical solutions. One of the codes was extended in order to provide some additional physical quantities of interest. This is done in section 5.

3. Introduction

In this section, we first introduce the motivation for fusion nuclear energy research. Afterwards, we give a brief discussion of the main problematics and current state of the research, and at the end we introduce the very basics of fusion reactions and power balance.

3.1 The role of fusion

Nowadays, it is unacceptable to think of a life without electricity, oil, or natural gas in the developed countries. However, the problematics associated with energy generation are not easy to solve. Fossil fuels are the principal source of energy of the world population by a large margin, yet the environmental complications related to them are becoming very significant. We also must consider that due to the population increase and the fast develop of highly populated countries like China or India will lead to a consequently higher demand of energy. Thus, we must face the problem of increasing the overall energy production while reducing our strong dependence on fossil fuels.

A lot of progress has been made in the last decades about this issue. On the one hand, nuclear fission power has become a significant source of electricity in the developed countries, contributing to the reduction of emissions of CO_2 and other pollutants to the atmosphere. On the other hand, the renewable energies development is also helping to solve this problem, with the added advantage that its environmental impact is even lower than the one of nuclear fission. These two alternatives to the fossil fuels are still not the final solution, since they also have very important disadvantages. Let’s consider nuclear fission first.

Nuclear fission technology is already well developed and established. The fuel necessary for the operation of nuclear reactors will still be available for a long time, and the power plants provide a continuous energy supply, but there are two environmental issues about fission power. One is the generation of radioactive waste,

which must be stored somewhere and may take up to hundreds of thousands of years until they are no longer hazardous to humans. The second problem is the inherent possibility of nuclear meltdown or other accidents. This is actually extremely rare and there is a lot of effort put in nuclear power plants security, but the danger is still there and the recent Fukushima accident (2011) has created a strong public rejection to fission power in many developed countries.

Renewable energies however have no important safety problems, nor produce dangerous waste, and the fuel is virtually unlimited and free, since most of them depend on the sun. Hydroelectric power plants make the most important contribution. It is a clean, fairly easy way to generate electricity, but has the important limitation that most of the suitable rivers for hydroelectric energy production are already exploited. In other words, the expansion perspectives here are very low. Wind and solar energy don't have this problem, but the power supply of both options is dependent on weather conditions, leading thus to a strong-fluctuating power supply. This together with the technological difficulties of storing energy makes them a not very attractive choice to be the basis of the world power supply.

This is where fusion power comes into play. No pollutants are emitted, almost no radioactive waste is generated, the fuel is extremely abundant and continuous operation should be possible. Moreover, the feared meltdown of the fission reactors is not possible in a fusion power plant, since the amount of fuel in the reactor is very low, and there is no chain reaction that can eventually grow uncontrolled. Actually, the fuel in a fusion reactor is in plasma state, this is a collection of electrons and ions which are too hot to form atoms or molecules. If this plasma expands and hit the first wall, it would be cooled and stop being a plasma, therefore nuclear reactions would immediately stop.

The main disadvantage of fusion is its complexity. There has been a lot of progress in the fusion research since the 50ies, when it started, but we are still some decades far away from having fusion-generated electricity into the grid. This doesn't mean that fusion is an unachievable dream. A large amount of fusion power was first achieved in 1991 in the experimental tokamak reactor JET [1], and net power is expected to be obtained in the on-going international project ITER.

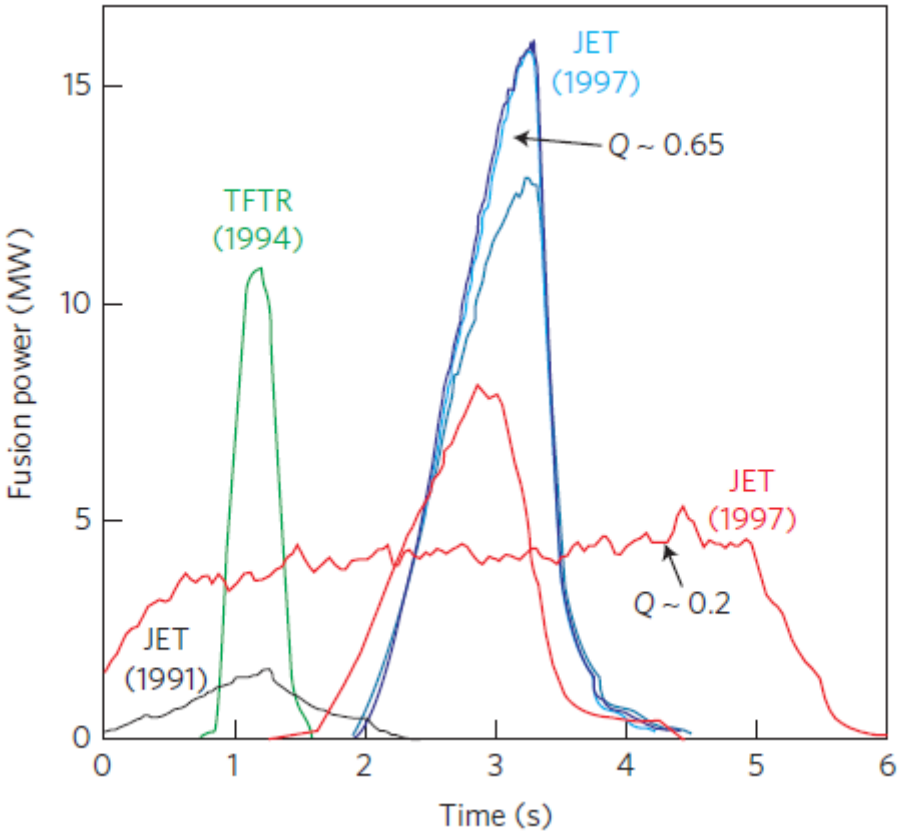

Figure 1. Fusion power achieved in JET and TFTR experiments in the 90ties. The fusion gain factor Q, defined as the output fusion power to the input power ratio, is shown. Image taken from reference 1.

Fusion is overall an excellent mid-term option to deal with the rising energy challenge and therefore the research and development towards a commercial fusion power plant must go on.

3.2 Tokamaks and H-mode

There are two main paths in the research of controlled thermonuclear fusion. One is the inertial confinement fusion (ICF), which consists of heating and compressing a tiny amount of D-T fuel using high energy lasers. The other one is the magnetic confinement fusion (MCF), where high intensity magnetic fields are used to hold the plasma together. We will focus on MCF in this work.

The magnetic confinement of the plasma is not an easy task. The most successful configuration at the moment is the tokamak, although stellarators, reversed field pinch experiments, and spheromaks are very interesting as well and under a lot of research. The tokamak is a donut-shaped reactor (a torus) in which there is a toroidal component of the magnetic field that provides fairly good perpendicular confinement while the parallel losses are avoided by the bending of the field lines over themselves. Actually, this is not enough to keep the plasma confined due to the drifts, as we will discuss later. The problem is solved by adding a poloidal component to the magnetic field. This poloidal field will usually be generated by a toroidal current flowing in the own plasma. Inducing this current is another difficult issue.

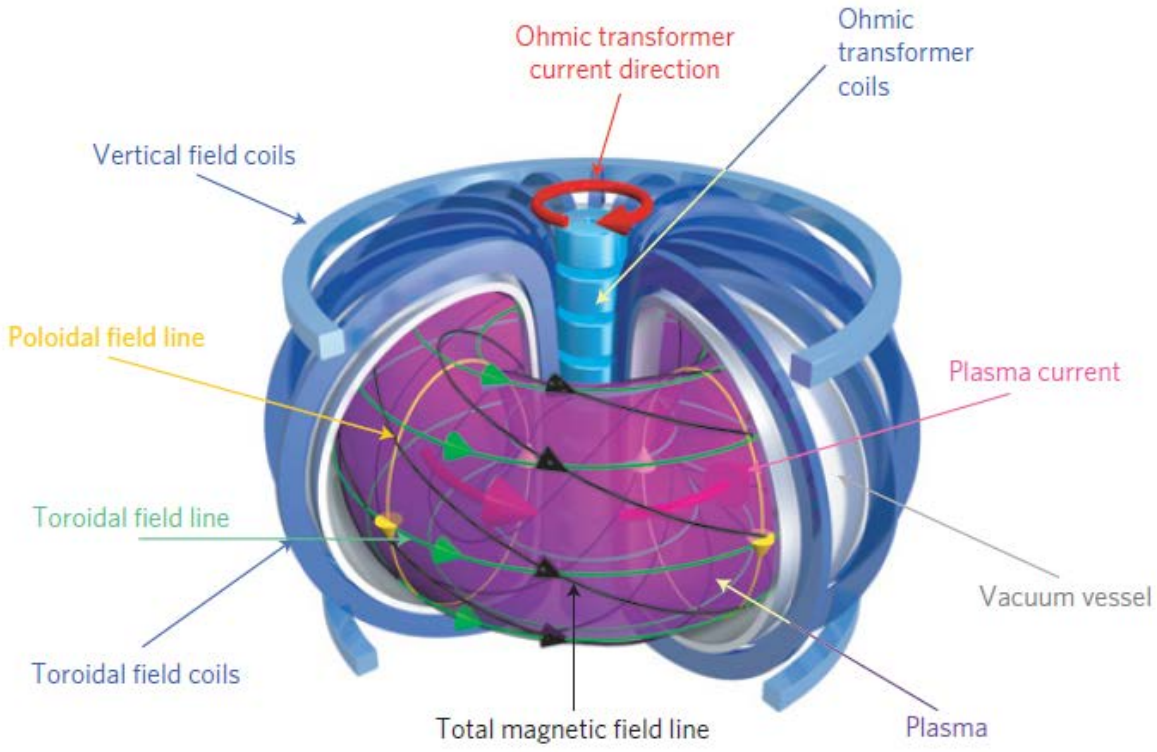

Figure 2. Schematic representation of the magnetic fields and current coils in a tokamak. Image taken from reference 1.

ITER, the biggest experimental nuclear fusion reactor ever built, will be a tokamak. Its main goal is to demonstrate the viability of fusion by going over the break-even value both under inductive and steady-state operation [2].

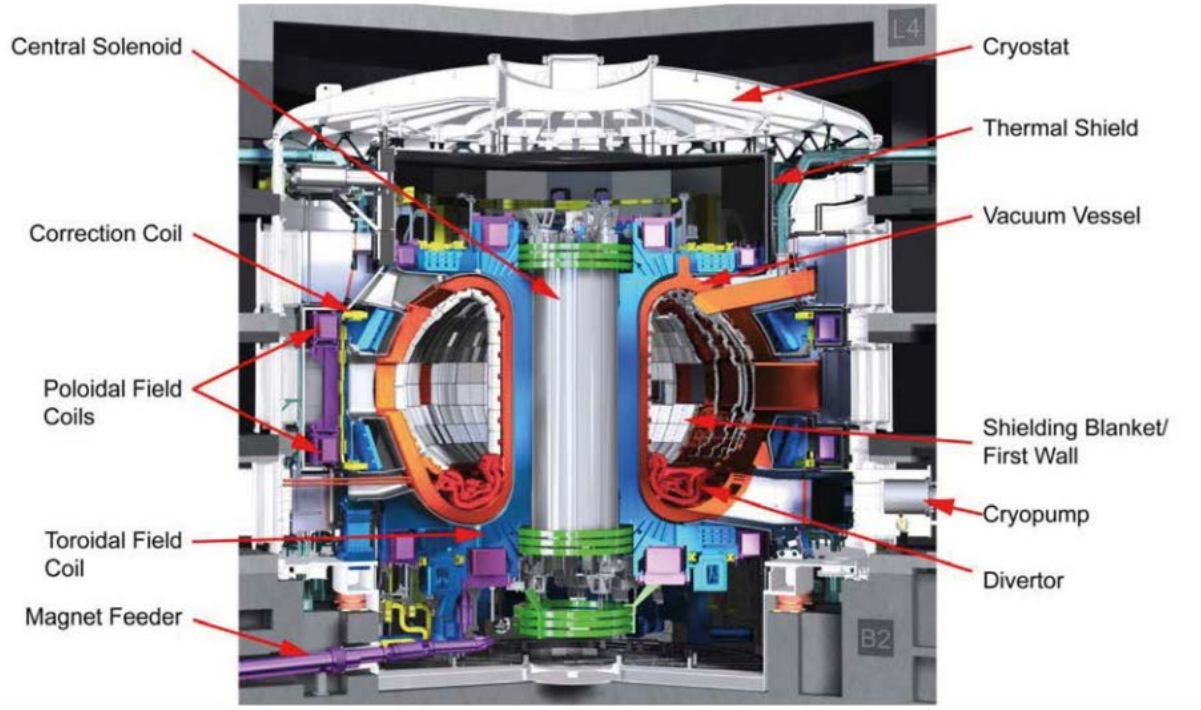

Figure 3. Cross section view of ITER reactor and its main components. The size of the whole reactor building will be of about 29m in diameter and height. Image from reference 2.

Some of the most critical components in tokamaks are the first wall, the blanket and the divertor. These are the three pieces of the tokamak that stand between the burning fusion plasma and the superconducting coils. In order to get an idea of what this implies, consider that in ITER the plasma will be at 150 million degrees kelvin and the superconducting coils will operate at 4K. ITER will actually be simultaneously one of the hottest and coldest places in the whole solar system.

The first wall is just the plasma facing side of the blanket. The design of the first wall is extremely important. In ITER, it will be made of beryllium in order to minimize the plasma contamination and it will be able to withstand heat fluxes of up to 4.7 MW/m^2. The blanket lies behind the first wall and will be used to slow down the fast neutrons coming from the fusion reactions and absorb its thermal energy by using water as a coolant. Another important goal of the blanket is to supply the tritium needed in the vacuum chamber. Although the blanket in ITER will not be able to breed the required tritium for the fusion reactions (at least at first), it is planned to do so in an actual fusion power plant.

The divertor is another plasma-facing, high technological component, just like the first wall. The difference is that the divertor will receive an even higher heat flux. In ITER, the divertor will be armored with tungsten and the heat flux on it will be of up to 20 MW/m^2.

Unfortunately, even with the clever magnetic configuration of tokamaks transport losses still greatly affect the plasma confinement. As the plasma gets heated, a collection of annoying instabilities appears, and the confinement time decreases. When the plasma is under a low temperature gradient regime, we say it operates in the low (L) confinement mode. All of the plasmas in the first tokamaks were always in this L-mode, and the situation got stuck for some time in magnetic confinement research [3]. A great improvement was made when the high (H) confinement mode was “discovered” in the ASDEX tokamak in 1982 [4]. This mode was reproduced in both tokamaks and stellarators afterwards and lead to the increase of the confinement time approximately by a factor of two. The transition from the L-mode to the H-mode is observed in most tokamak experiments when the external heating reaches a certain threshold.

The H-mode, however, is not a final perfect solution for magnetic confinement in tokamaks. A lot of transport losses due to instabilities such as the so-called Edge Localized Modes (ELM) were still presents, and further research ended up in the very high (VH) mode and the improved (I) mode, both discovered in the 90ies. Much progress has been made on this subject, but research is still going on. ITER will be a key step in the study of magnetic confinement. It will operate mainly under H-mode regime, but other scenarios such as the I-mode will also be taken into consideration. Another issue worth to mention about the H-mode is that its underlying physics are not well understood yet. Some researchers have pointed out that the L-H transition is actually very similar to a second order Landau phase transition [5], but a fully theoretical explanation is not given at the moment. Only empirical formulas based on experimental evidence from tokamak and stellarator experiments have been proposed, in order to give the threshold input power at which the L-H transition occurs.

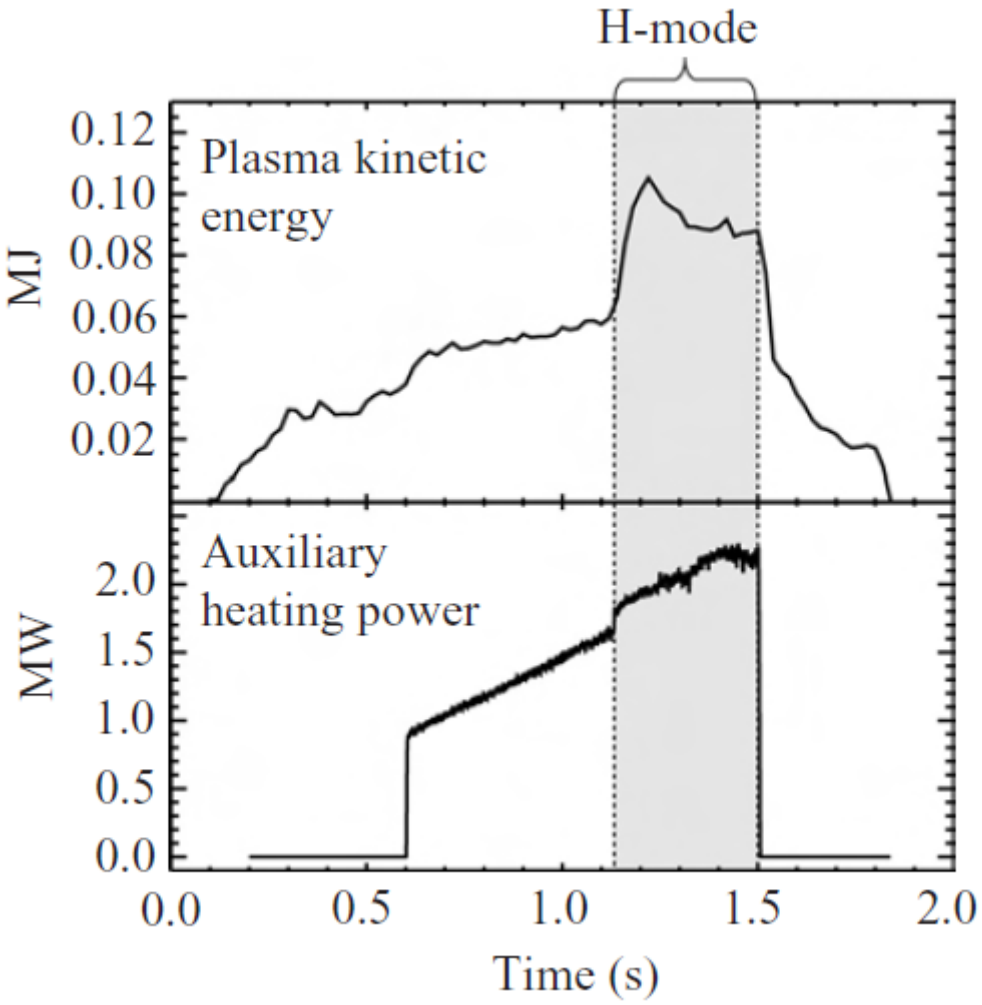

Figure 4. Experimental evidence of the H-mode existence when the auxiliary heating power reaches a certain threshold. Image taken from reference 7.

Stellarators, on the other hand, do not rely on the toroidal plasma current to induce the poloidal component of the magnetic field. The magnetic field in this case is entirely generated by external coils. The resulting magnetic field is no longer axisymmetric and therefore an additional dimension is added to the balance equations, which of course makes them more difficult to solve. This complicates a lot the geometry and design of the reactor but, due to the absence of plasma current, the stability of the plasma is greatly improved compared to tokamaks. The most modern stellarator experiment nowadays is the Wendelstein 7-X (W7-X), located in Germany. Stellarators may overpass tokamaks performance in the future, but for the moment they are farther away from reaching commercial fusion.

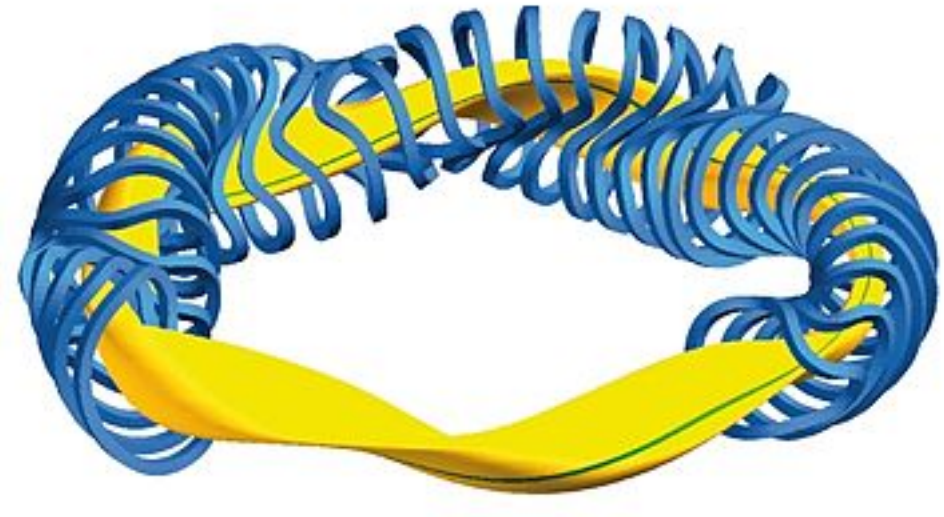

Figure 5. Representation of the complex coil distribution (blue), plasma shape (yellow), and a particular magnetic field line (green) in a stellarator. Image from Wikipedia.

Another option of interest in current research is the reversed field pinch (RFP) configuration. These are also axisymmetric toroidal devices, but they differ from tokamaks in the magnetic configuration they use. In RFP experiments, unlike in tokamaks, the toroidal component of the magnetic field changes its value along the radial axis, and eventually reverse its direction (hence its name). A very attractive characteristic of this device is that they are able to operate under kink safety factor $q_* < 1$ (this magnitude is related to the relative intensity of the toroidal magnetic field to the poloidal magnetic field), which is not possible in tokamaks, that would suffer kink instabilities that would quickly disrupt the confinement [6]. This is helpful in order to achieve high beta[1] ($\sim 10\%$) plasmas, which ultimately turns in a higher power output from the reactor. The main disadvantage of RFP configurations is that non-linear effects and turbulences are more significant than in tokamaks.

Spheromaks are toroidal confinement devices too, but they lack of any toroidal field coils, which results in a toroidal magnetic field of the same order of magnitude as the poloidal field. They also present extremely small *aspect ratios* $1/\varepsilon = R_0/a \sim 1$ and, theoretically, should be able to reach ignition in the future by only ohmic heating, since their projected plasma current is much larger than that of the tokamaks. These characteristics reduce a lot the capital cost of spheromaks in comparison with

[1] Beta stands for the normalized pressure of the plasma, as we will define more in detail in section 5.

tokamaks (especially due to the absence of toroidal super-conducting coils) Their main problems are related to stability and transport, and the plasma physics knowledge in spheromaks is far behind the understanding of tokamak plasmas, so we will have to wait some decades to see if the spheromak concept is really valid for a fusion power plant.

Since the physics of tokamak plasmas are much better understood than that of the other magnetic confinement concepts, we will focus on tokamaks from now on, with the only exception of sections 5.3 and 5.4.

3.3 Fusion reaction basics

This section will cover the basics of the fusion reaction investigated in present research, including a simple power balance analysis in order to have some basic understanding of the current state of fusion research, which will be briefly discussed at the end of the section. The physical concepts developed in what follows will be mainly based, unless specified, in reference [7].

In a nuclear reaction, the difference of mass of the final particles respect to the initial particles yields the energy liberated (or consumed) in the reaction. For fusion reactions, due to the form of the binding energy curve, the most suitable nucleons are the lightest ones, i.e. the isotopes of hydrogen and helium.

The easiest fusion reactions to initiate would be the ones in which a neutron merges with a nucleus. The problem with these reactions is that they don’t give rise to more neutrons, and since there is no effective source of neutrons, they are not a valid choice.

We must therefore evaluate the fusion of light elements. In this case, the coulomb potential barrier must be overcome, which means that very high energies will be needed in order to make the reactions possible. Out of the various existing options, the easiest reaction to initiate is deuterium (D) – tritium (T) fusion.

$$D + T \rightarrow \alpha + n + 17.6\ \text{MeV}.$$

The cross section of this reaction is compared to D-^{3}He and D-D fusion in figure 6. The energy liberated is distributed between the alpha particle (3.5 MeV) and the neutron (14.1 MeV) in the form of kinetic energy. Alpha particles will help in the warming of the plasma while neutrons will escape to the blanket and constitute the main source of energy in the reactor. There is however no natural tritium in Earth due to its short half-life. This means that the tritium will have to be supplied by means of the following reactions

$$Li^{6} + n \rightarrow \alpha + T + 4.8\ \text{MeV},$$

$$Li^{7} + n \rightarrow \alpha + T + n - 2.5\ \text{MeV}.$$

Even though Li^{7} is far more common than Li^{6}, it is the Li^{6} reaction the one that will mainly provide the tritium in a reactor, because it is much easier to initiate.

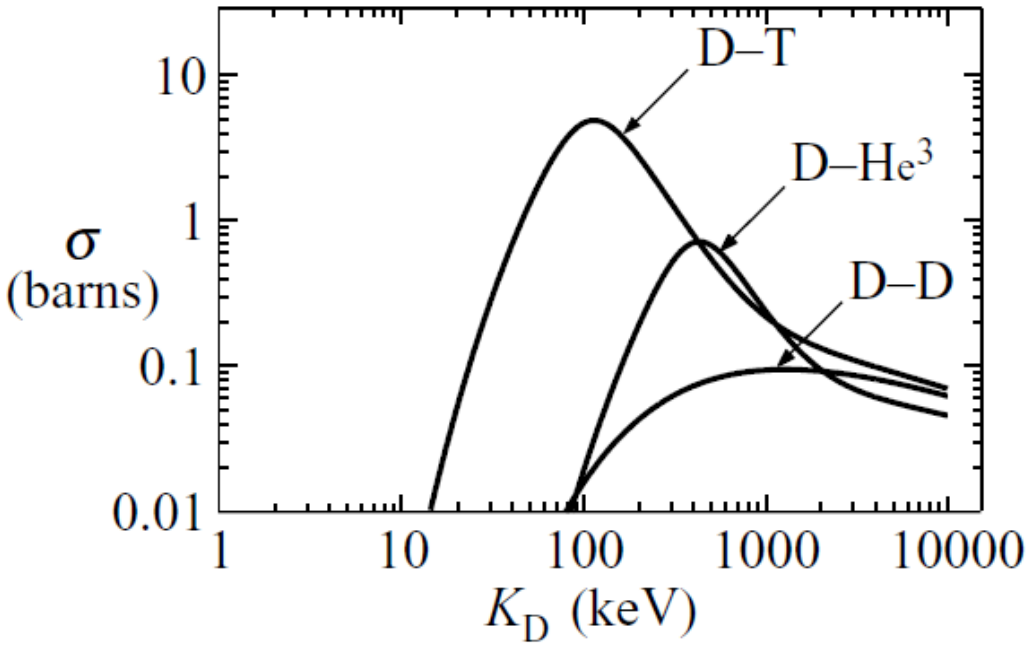

Figure 6. Experimental cross sections for different fusion reactions as a function of the interaction energy (in this case the deuteron energy). D-T fusion has by far the highest cross section. Image taken from reference 7.

3.4 Conservation of energy and power balance

The fusion reaction rate R_{12} is defined as the number of D-T collisions per unit volume per unit time. If each fusion collision generates an energy E_f we can define the fusion power density S_f as

$$S_f = E_f \, R_{12}. \tag{1}$$

The calculation of the reaction rate requires the introduction of distribution functions $f(\boldsymbol{r}, \boldsymbol{v}, t)$. If $f_1(\boldsymbol{r_1}, \boldsymbol{v_1}, t)$ is the deuterium nuclei distribution function and $f_2(\boldsymbol{r_2}, \boldsymbol{v_2}, t)$ the tritium nuclei distribution function, we can write the reaction rate as

$$R_{12} = \int f_1(\boldsymbol{v_1}) \, f_2(\boldsymbol{v_2}) \, \sigma(\boldsymbol{v}) \, \boldsymbol{v} \, d\boldsymbol{v_1} \, d\boldsymbol{v_2} = n_1 n_2 < \sigma v >. \tag{2}$$

where $\boldsymbol{v}$ is the relative velocity of the particles and we assumed the densities n_1 and n_2 are homogeneous. Assuming both densities are equal and that the plasma is neutral, that is $n_1 + n_2 = n_e$, the fusion power density is

$$S_f = \frac{1}{4} E_f \, n_e^2 < \sigma v >. \tag{3}$$

In order of a nuclear fusion to occur, the particles have to overcome the Coulomb barrier. Let's take first a classical approach. If we consider a nuclear collision in the center of mass frame in which the kinetic energies of the deuterium and tritium nucleus are T_D and T_T respectively, and their diameter is d, the following condition must be fulfilled

$$T_D + T_T \geq \frac{e^2}{4\pi\varepsilon_0 d}. \tag{4}$$

which can be written in terms of the reduced mass $m_r = m_D m_T/(m_D + m_T)$ and the relative velocity v

$$\frac{1}{2} m_r v^2 \geq \frac{e^2}{4\pi\varepsilon_0 d} \approx 288 \text{ KeV}. \tag{5}$$

So, in classical physics, no fusion will occur at lower interaction energies. If we take quantum mechanical effects into account things get much better. First thanks to the tunnel effect reactions may take place at much lower interaction energies, with a given probability. Second, if the nuclei velocity is too large, they may pass through one another without undergoing a fusion process. And third, under some specific conditions the colliding nuclei may exhibit a resonance, giving rise to a higher probability of going through a nuclear fusion and therefore increasing the cross section.

The combined result of these effects results in the maximum cross section being at only $120\ \mathrm{KeV}$ of interaction energy. This implies that the required temperature of the fuel will be of the order of $T \sim 10\mathrm{KeV}$, at which the D-T mixture is fully ionized and thus constitute a plasma. Please note that from now on I will refer to T as $k_B T$, i.e. T will be measured in units of energy, as it is usually done in plasma physics.

In fusion plasmas, the gained energy from the fusion reactions has to balance the power losses due to radiation. This is one important, inevitable procedure that always affects the power balance. The most important radiation losses mechanism is *Bremsstrahlung* radiation. When a non-relativistic electron experiments a coulomb collision with an ion, it slows down and emits ultraviolet or X-ray radiation according to

$$P = \frac{\mu_0 e^2 \dot{v}^2}{6\pi c}. \tag{6}$$

The total power density associated to this phenomenon is

$$S_B = C_B n_e^2 T_e^{1/2}, \tag{7}$$

with $C_B = \mathrm{const}$.

Hereafter we assume the fuel is a 50%-50% D-T mixture with very few alpha particles, each component has the same temperature and it is an ionized gaseous plasma near thermodynamic equilibrium. This means that we can use the known relations $U_j = \frac{3}{2} n_j T_j$ and $p_j = n_j T_j$, So that the total the total energy density is given by

$$U = U_D + U_T + U_e = 3nT = \frac{3}{2}p, \tag{8}$$

where p is the total pressure.

Now we take the following formula for the conservation of energy in fluid dynamics

$$\frac{3}{2}\frac{\partial p}{\partial t} + \frac{3}{2}\nabla \mathrm{p}\boldsymbol{v} + p\nabla\boldsymbol{v} + \nabla\boldsymbol{q} = S, \tag{9}$$

where the $\nabla\boldsymbol{q}$ term represents the diffusive process due to heat conduction. We will assume for the present analysis that the plasma is under steady state conditions, and we will also neglect the convection and compression terms. Taking into account that the power density S is the sum of the fusion power density $S_{\boldsymbol{f}}$, the Bremsstrahlung radiation power density S_B and the external power density S_h, we can write

$$\nabla\boldsymbol{q} = S = S_{\boldsymbol{f}} - S_B + S_h. \tag{10}$$

We now must define *the energy confinement time* (or simply confinement time) τ_E, a very important quantity in fusion plasmas, as

$$\frac{1}{V}\int_V \boldsymbol{\nabla q}\, \boldsymbol{dr} = \frac{3}{2}\frac{p}{\tau_E}. \tag{11}$$

The confinement time is the relaxation time of the plasma due to heat conduction. For a fusion reactor, a high confinement time is desired. Improving this critical parameter is one of the ultimate goals of fusion plasma physics, in particular of magnetic fusion confinement research. Unfortunately, the typical values of the confinement time in an experimental fusion reactor are only of the order of one second.

Now we are in position to write the so called 0-D conservation of energy as

$$\frac{E_\alpha}{16}p^2\frac{<\sigma v>}{T^2} + S_h = \frac{C_B}{4}\frac{p^2}{T^{3/2}} + \frac{3}{2}\frac{p}{\tau_E}. \tag{12}$$

Note that hereafter we will refer to the fusion energy liberated in a fusion collision as $E_f \rightarrow E_\alpha$, since only alpha particles contribute to the power balance of the plasma.

If the alpha power is able to heat the plasma compensating thermal conduction and radiation losses, we need no longer external power, which means that the fusion reaction is self-sustaining. This point is known as ignition. Mathematically this means

$$S_\alpha = S_B + S_\kappa. \tag{13}$$

After rearranging the terms and taking into account that the minimum temperature for ignition is about 15 KeV, we get

$$p\tau_E \geq 8{,}3 \text{ atm s}. \tag{14}$$

This condition is known as *the Lawson criterion*, and of course has not yet been achieved in any experimental fusion reactor. There is however a progression in the experimental reactors towards the Lawson curve, and hopefully it may be reached in the future. It is important to define another parameter known as the *gain factor* Q as

$$Q = \frac{P_{out} - P_{in}}{P_{in}}. \tag{15}$$

The previously discussed ignition state would correspond to an infinite value of Q. In actual experimental reactors Q has always been below one, which means that the break-even value ($P_{out} = P_{in}$) has not been achieved yet. Fortunately, ITER is expected to greatly surpass this value with $Q = 10$ under inductive operation and $Q = 5$ under steady-state operation [8]. In particular, it is designed to produce 500 MW of output power with 50 MW of input power. We are still a long way far away from ignition, but it seems that we are in the right way.

4. MHD

The most accurate model to describe plasmas is kinetic theory. However, we are going to focus here in a simpler, more intuitive model known as magnetohydrodinamics (MHD). In this section we aim to obtain the equilibrium relation given by this model, the Grad-Shafranov equation.

4.1 MHD equations

The simplest self-consistent description of a plasma is given by the MHD equations. These are a set of relations that describe a plasma by means of a single fluid model coupled to the Maxwell equations. Despite its simplicity, it allows one to obtain good qualitative and quantitative results and, in particular, it is accurate enough to describe equilibrium of fusion plasmas. After assuming the quasi-neutrality of the plasma and considering the time and length scale hierarchy of the different processes in plasmas, one can show [7] that the MHD equations are the ones given in table 1.

Table 1. MHD equations.

Mass conservation	$\frac{d\rho}{dt} + \rho\nabla \cdot \boldsymbol{v} = 0$
Momentum conservation	$\rho\frac{d\boldsymbol{v}}{dt} = \boldsymbol{J} \times \boldsymbol{B} - \nabla p$
Ohm's law	$\boldsymbol{E} + \boldsymbol{v} \times \boldsymbol{B} = \eta_{\parallel}\boldsymbol{J}$ (resistive) $\boldsymbol{E} + \boldsymbol{v} \times \boldsymbol{B} = 0$ (ideal)
Energy conservation	$\frac{d}{dt}\left(\frac{p}{\rho^{5/3}}\right) = 0$
Maxwell equations	$\nabla \times \boldsymbol{E} = -\frac{\partial \boldsymbol{B}}{\partial t}$ $\nabla \times \boldsymbol{B} = \mu_0\boldsymbol{J}$ $\nabla \cdot \boldsymbol{B} = 0$

Where ρ is the mass density of the plasma, $\boldsymbol{v}$ is the macroscopic velocity, $\boldsymbol{J}$ is the current density, p is the plasma pressure, $\eta_{\parallel}$ is the parallel resistivity and $\boldsymbol{E}$ and $\boldsymbol{B}$ are the electric and magnetic field, respectively.

4.2 MHD equilibrium

The goal of this section is to apply the ideal MHD equations to an actual fusion problem and analyze the results. More exactly, we will be interested in MHD equilibrium, which means that we are going to look for steady state solutions to the MHD equations. This condition simplifies the set of relations presented before by making all the time derivatives and velocities equal to zero. The remaining non-trivial equations are the following:

$$\boldsymbol{J} \times \boldsymbol{B} = \nabla p \tag{16}$$

$$\nabla \times \boldsymbol{B} = \mu_0 \boldsymbol{J} \tag{17}$$

$$\nabla \cdot \boldsymbol{B} = 0. \tag{18}$$

Equations (17,18) are just Maxwell equations and equation (16) describes the force balance in the plasma. We are interested only in physical solutions that correspond to a well confined plasma. Several possible mathematical solutions for the pressure are illustrated in figure 7.

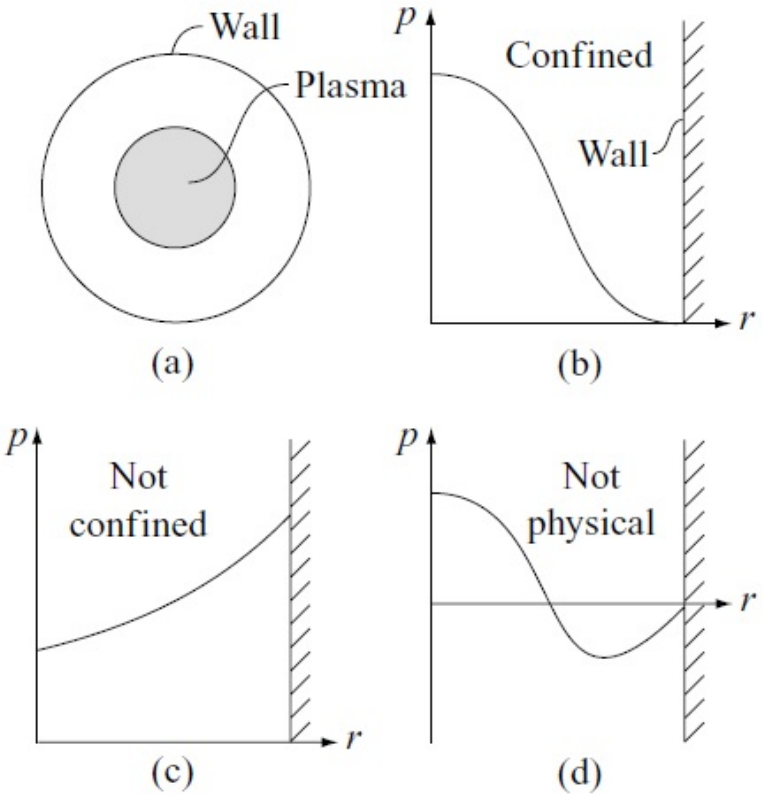

Figure 7. (a), (b) Schematic representation and suitable pressure profile of the desired equilibrium. (c) Pressure profile corresponding to an unacceptable equilibrium. (d) Solution of no physical interest. Image from reference 7.

Taking the scalar product of the magnetic field or the current density times equation (16) we find that both the magnetic field lines and the current density are perpendicular to the pressure gradient. In other words, the magnetic field lines lie on a series of constant pressure, nested toroidal surfaces. These surfaces are called flux surfaces.

The force balance issue can be divided in radial force balance and toroidal force balance. If we were able to unbend the torus into a cylinder there would only be radial force balance, and due to the bending into a torus an additional outwards force appears. In order to accomplish the desired equilibrium, the simplest configurations that one could try are a poloidal current induced by a toroidal field (that is, a θ pinch) or a toroidal current induced by a poloidal field (a Z pinch). Both are able to provide radial force balance, but none of them are actually suitable for a good plasma confinement. The θ pinch has a bad toroidal equilibrium, but it is adequate in terms of stability. The Z pinch behaves the opposite way; it has a good toroidal equilibrium but bad stability.

The solution is obviously to take a combination of both configurations, what is known as a screw pinch. In this case, the magnetic field lines wrap like a helix around the torus.

4.3 Grad-Shafranov equation

Here we will derive one of the most important equations in fusion plasma physics, the Grad-Shafranov equation. The procedure will be mainly based on the one used by Boyd [9]. The description of the toroidal force balance in a general screw pinch is an important issue. If we assume an axisymmetric toroidal geometry, using cylindrical coordinates R, ϕ, Z and $\boldsymbol{B} = \nabla \times \boldsymbol{A}$ we find that

$$\boldsymbol{B} = -\frac{1}{R}\frac{\partial \Psi}{\partial Z}\boldsymbol{e_R} + B_\phi \boldsymbol{e_\phi} + \frac{1}{R}\frac{\partial \Psi}{\partial R}\boldsymbol{e_Z}. \tag{19}$$

Here Ψ is the flux function, which is related to the toroidal component of the vector potential $A_\phi = \psi/R$ and to the poloidal magnetic flux Ψ_p going through the surface bounded by a given R and $Z = 0$, by $\Psi_p = 2\pi\Psi$. Using (19) and the fact that due to

axial symmetry the flux function does not depend on ϕ, one can show that $\boldsymbol{B} \cdot \nabla\Psi = 0$. The constant flux surfaces are also the surfaces generated by the magnetic field lines. From now on we will refer to Ψ to label the flux surfaces. This expression for the magnetic field in terms of the toroidal component and the flux function can be used together with equations (16) and (18) to get

$$\mu_0 \frac{\partial p}{\partial Z} + B_\phi \frac{\partial B_\phi}{\partial Z} + \frac{1}{R^2}\frac{\partial \Psi}{\partial Z}\Delta^*\Psi = 0. \tag{20}$$

Where the elliptic operator Δ^* is defined as

$$\Delta^* = \frac{\partial^2}{\partial R^2} - \frac{1}{R}\frac{\partial}{\partial R} + \frac{\partial^2}{\partial Z^2}. \tag{21}$$

As we already know, the flux surfaces are isobaric surfaces and hence $p = p(\Psi)$. It can also be shown that $\nabla\Psi \times \nabla(RB_\phi) = 0$, so the flux surfaces are also surfaces of constant RB_ϕ, which motivates us to introduce the function $RB_\phi = F(\Psi)$. This function is related to the net poloidal current flowing in the plasma and the external field coils $I_p(\Psi)$ by $2\pi F(\Psi) = \mu_0 I_p(\Psi)$. The final step is to rewrite equation (20) in terms of these unknown functions:

$$\Delta^*\Psi + F\frac{dF}{d\Psi} + \mu_0 R^2 \frac{dp}{d\Psi} = 0. \tag{22}$$

This is the well-known Grad-Shafranov (GS) equation, which describes the toroidal force balance for axisymmetric plasmas. This is in general a two-dimensional, non-linear elliptic partial differential equation for the flux function Ψ, which is both a dependent and independent variable.

Let's analyze the meaning of each term in the GS equation. The first term in the equation comes from the poloidal component of the magnetic field and it is necessary to ensure toroidal stability (θ pinch). The second accounts for the toroidal magnetic field, essential for radial stability (Z pinch). Finally, the third term represents the pressure gradient expanding force, which balances with the other two terms.

In order to solve this equation, one needs to specify the exact form of the two unknown functions $p(\Psi)$ and $F(\Psi)$ together with the boundary conditions.

5. Equilibrium in fusion plasmas

In this final section, we find and study the results of the Grad-Shafranov equation. We also look for equilibrium states by means of Taylor states, as it will be explained later.

5.1 Solov'ev equilibrium: Theory

There are several methods in the literature to solve the GS equation. The most direct and general approach is to look for a numerical solution. However, we will consider here other procedures that look for analytical solutions of the GS equation. These solutions are usually a linear combination of an infinite number of terms, from which we will only retain some. This will allow us to determine an approximate analytical solution given by some unknown coefficients. These coefficients will be determined by choosing suitable boundary conditions and taking advantage of the software MATLAB.

The first method we will consider to solve the GS equation is based on reference [10]. This method will allow us to calculate the flux surfaces for up-down symmetric equilibria for a given set of geometrical parameters, which is different for each experimental device. Furthermore, up-down asymmetric equilibria with an X-point can also be solved by adding the location of the X-point and some additional constraints but, for the sake of simplicity, we will focus on the up-down symmetric case.

The first step to solve the GS equation is to use non-dimensional magnitudes by defining $R = R_0 x$, $Z = R_0 y$, and $\Psi = \Psi_0 \psi$, where we use the major radius of the plasma R_0 for the spatial scaling and Ψ_0 is an arbitrary constant. In terms of these new dimensionless variables, the GS equation becomes

$$x \frac{\partial \psi}{\partial \mathrm{x}} \left(\frac{1}{x} \frac{\partial \psi}{\partial \mathrm{x}} \right) + \frac{\partial^2 \psi}{\partial \mathrm{y}^2} = -\mu_0 \frac{R_0^4}{\Psi_0^2} x^2 \frac{dp}{d\psi} - \frac{R_0^2}{\Psi_0^2} F \frac{dF}{d\psi}. \tag{23}$$

The form of the unknown functions p and F is chose such that the GS equation turns into a linear inhomogeneous partial differential equation, making it much easier to solve. This is the so called Solov'ev equilibrium. The linearization is ensured by the following choice of p and F

$$-\mu_0 \frac{R_0^4}{\Psi_0^2}\frac{dp}{d\psi} = C \qquad -\frac{R_0^2}{\Psi_0^2}F\frac{dF}{d\psi} = A. \tag{24}$$

With A and C being constant that, without loss in generality (since Ψ is an arbitrary, free constant), can be chosen so that $A + C = 1$. The resulting form of the GS equation is

$$x\frac{\partial\psi}{\partial \mathrm{x}}\left(\frac{1}{x}\frac{\partial\psi}{\partial \mathrm{x}}\right) + \frac{\partial^2\psi}{\partial \mathrm{y}^2} = (1-A)x^2 + A. \tag{25}$$

The problem has been greatly simplified. This equation can actually be solved analytically and be evaluated for a given value of the parameter A, which is related to the normalized pressure β of the plasma. This is a very important quantity in fusion plasmas and it is defined as the ratio of the average plasma pressure to the magnetic pressure

$$\beta = \frac{2\mu_0\langle p\rangle}{B_0^2 + \bar{B}_p^2}. \tag{26}$$

Here, the magnetic field B^2 term has been written in terms of its toroidal (B_0^2) and average poloidal ($\bar{B}_p^2$) component. In order to get a higher fusion power output in a reactor, a high β is desirable. Unfortunately, as beta increases, the plasma becomes extremely unstable and cannot be sustained. This fixes an upper limit of beta, which can be improved by using plasmas with a non-circular toroidal cross section. In fact, all modern tokamaks rely on D-shaped plasmas rather than circular plasmas. In particular, a way to increase the highest allowed beta in a tokamak is by using an elliptical toroidal cross section shape. The ellipticity is characterized by *the elongation* κ ($\kappa = 1$ is a circle). Also, in order to build an effective divertor tokamak, an elongated plasma shape is necessary.

The general solution of an inhomogeneous equation is the combination of a particular solution and the general solution to the associated homogeneous equation. A particular solution to (25) is

$$\psi_p(x,y) = \frac{x^4}{8} + A\left(\frac{1}{2}x^2 \ln x - \frac{x^4}{8}\right). \tag{27}$$

The solution to the inhomogeneous equation is an infinite some of polynomial terms [11]. Here we will consider only the terms up to x^6 and y^6. The final, general solution is thus

$$\psi(x,y) = \frac{x^4}{8} + A\left(\frac{1}{2}x^2 \ln x - \frac{x^4}{8}\right) + c_1\psi_1 + c_2\psi_2 + c_3\psi_3 + c_4\psi_4 + c_5\psi_5 + c_6\psi_6 + c_7\psi_7. \tag{28}$$

Where the functions ψ_i are known polynomial terms,

$$\begin{gathered} \psi_1 = 1 \qquad \psi_2 = x^2 \qquad \psi_3 = y^2 - x^2 \ln x \qquad \psi_4 = x^4 - 4x^2y^2 \\ \psi_5 = 2y^4 - 9y^2x^2 + 3x^4 \ln x - 12x^2y^2 \ln x \\ \psi_6 = x^6 - 12x^4y^2 + 8x^2y^4 \\ \psi_7 = 8y^6 - 140y^4x^2 + 75x^4y^2 - 15x^6 \ln x + 180x^4y^2 \ln x \\ - 120x^2y^4 \ln x, \end{gathered} \tag{29}$$

and the coefficients c_i are determined by the boundary conditions for ψ. In order to find these constraints, we consider that the toroidal cross section of the plasma is given by the following parametric equations

$$x = 1 + \varepsilon\cos(\tau + \alpha\, sin\,\tau) \qquad y = \varepsilon\kappa \sin\tau, \tag{30}$$

where $0 \le \tau \le 2\pi$, and we define the geometric parameters characteristic of fusion plasmas as $\varepsilon = a/R_0$ the inverse aspect ratio, κ the elongation and $\sin\alpha = \delta$ *the triangularity*. The definition of these geometric parameters is graphically explained in figure 8.

The following boundary conditions are imposed on the three marked points in figure 8. Note that, due to the axi-symmetry, we do not need to impose these conditions on the point symmetrical to the high point.

$$\psi(1+\varepsilon, 0) = 0$$
$$\psi(1-\varepsilon, 0) = 0$$
$$\psi(1-\delta\varepsilon, \kappa\varepsilon) = 0$$

$$\frac{\partial \psi}{\partial x}(1-\delta\varepsilon, \kappa\varepsilon) = 0$$
$$\frac{\partial^2 \psi}{\partial y^2}(1+\varepsilon, 0) = \frac{(1+\alpha)^2}{\varepsilon\kappa^2}\frac{\partial \psi}{\partial x}(1+\varepsilon, 0) \tag{31}$$
$$\frac{\partial^2 \psi}{\partial y^2}(1-\varepsilon, 0) = -\frac{(1-\alpha)^2}{\varepsilon\kappa^2}\frac{\partial \psi}{\partial x}(1-\varepsilon, 0)$$
$$\frac{\partial^2 \psi}{\partial x^2}(1-\delta\varepsilon, \kappa\varepsilon) = \frac{\kappa}{\varepsilon \cos^2\alpha}\frac{\partial \psi}{\partial y}(1-\delta\varepsilon, \kappa\varepsilon)$$

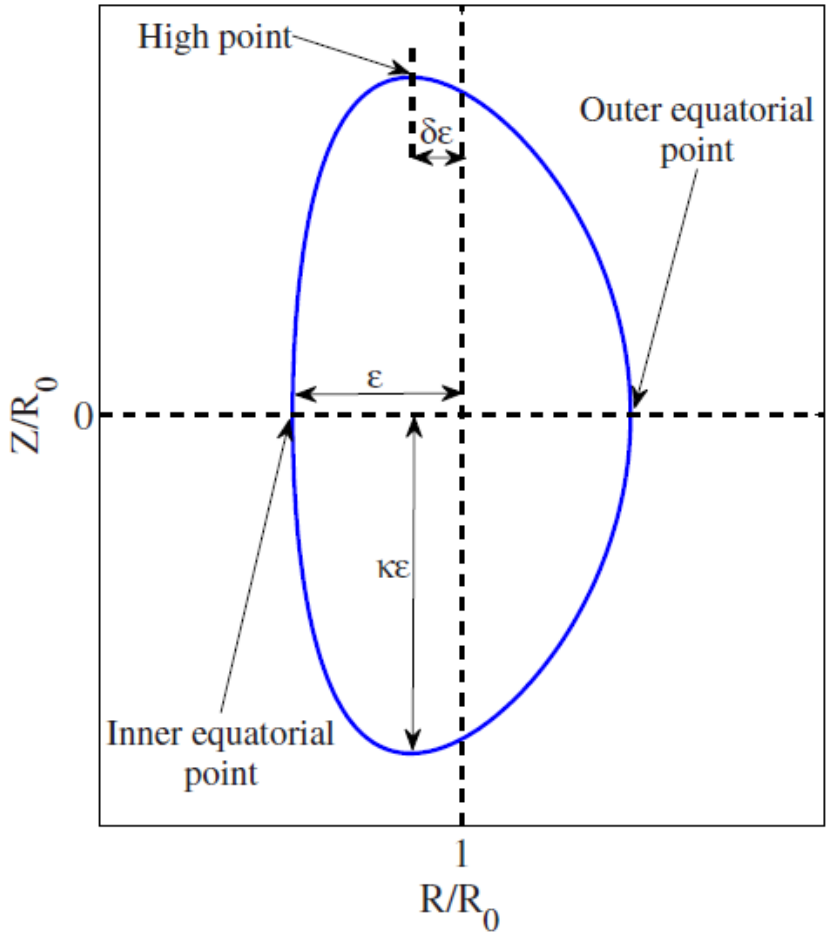

Figure 8. Definition of the geometrical parameters ε, κ, and δ, as well as the definition of the three critical points that will be used in the boundary conditions. Image taken from reference 9.

These conditions guarantee that the plasma edge (which is limited by one last closed flux surface, also called separatrix) matches the border previously defined and that its curvature is smooth. We are left with a system of 7 algebraic equations with 7 unknown coefficients. This will be easily solved by a MATLAB code, closing the problem.

In summary, the code associated to this article [10] calculates the flux function in all space, and plot its relevant surfaces (up to the separatrix), leaving the geometrical parameters ε, κ, and δ as free parameters to specify. The constant A remains as a parameter as well, although it is strongly related to the toroidal magnetic field and the pressure through the constant Ψ_0^2 (see equations 24), and it is decisive to determine the beta regime of the plasma whose flux surfaces are calculated.

As an expansion added to the code, we can also calculate the toroidal beta β_t, poloidal β_p, and total beta β, related by

$$\frac{1}{\beta} = \frac{1}{\beta_t} + \frac{1}{\beta_p}. \tag{32}$$

In order to perform these calculations, we first have to define the normalized poloidal circumference C_p and the normalized plasma volume V as

$$\begin{aligned} C_p &= \frac{1}{R_0}\oint dl_p = 2\int_{1-\varepsilon}^{1+\varepsilon} \sqrt{\left[1+\left(\frac{dy}{dx}\right)^2\right]}\, dx \\ V &= \frac{1}{2\pi R_0^3}\int d\mathbf{r} = \int x\, dxdy. \end{aligned} \tag{33}$$

We also have to add the kink safety factor q_* as an input. Its value can be either imposed or estimated through the following relation

$$q_* = \frac{\varepsilon R_0 B_0 C_p}{\mu_0 I_\phi}, \tag{34}$$

where I_ϕ is the toroidal current. In actual tokamak experiments this is just the plasma current. Also, taking advantage of the linear dependence of p and F with ψ, we can integrate equations (24) to get

$$p(x,y) = -\frac{\Psi_0^2}{\mu_0 R_0^4}(1-A)\psi \tag{35}$$

$$B_\phi^2(x,y) = \frac{1}{x^2}\left(B_0^2 - \frac{2\Psi_0^2}{R_0^4}A\psi\right). \tag{36}$$

Since the flux function ψ takes negative values inside the plasma, if want the pressure to be positive then the value of A is limited by $A \leq 1$. For other values of A, our calculations would have no physical meaning. Moreover, when the flux function $\psi = 0$, then the pressure becomes zero too, and when A decreases, the pressure increases. The value of the constant Ψ_0 can be obtained from the safety factor relation with ψ

$$\Psi_0 = \frac{-\varepsilon R_0^2 B_0 C_p}{q_* \int \frac{dxdy}{x}[A + (1-A)x^2]}. \tag{37}$$

Here the integral is done over the defined poloidal cross section surface. Now we can write the three betas of eq. (32) in terms of known parameters and the flux function

$$\beta_p = -2(1-A)\frac{C_p^2}{V}\frac{\int \psi\, x\, dxdy}{\left\{\int \frac{dxdy}{x}[A + (1-A)x^2]\right\}^2} \tag{38}$$

$$\beta_t = \frac{\varepsilon^2 \beta_p}{{q_*}^2} \tag{39}$$

$$\beta = \frac{\varepsilon^2 \beta_p}{{q_*}^2 + \varepsilon^2}. \tag{40}$$

The calculation of the betas is crucial in order to know what the plasma operating regime is for a given A. We are now in a position to evaluate the code for different characteristic geometrical parameters and different values of A.

5.2 Solov'ev equilibrium: Results

We will begin by studying the flux surfaces obtained with a set of geometrical parameters consistent with ITER. These are given in the MATLAB code, and their values are $\varepsilon = 0.32$, $\kappa = 1.7$, and $\delta = 0.33$. We can start by choosing the extremum value $A = 1$, which correspond to a zero pressure plasma, often referred to as "force free" plasma. The resulting flux surfaces are illustrated in figure 9. The most external flux surface will, in general, correspond to zero pressure, which means that it represents the plasma border.

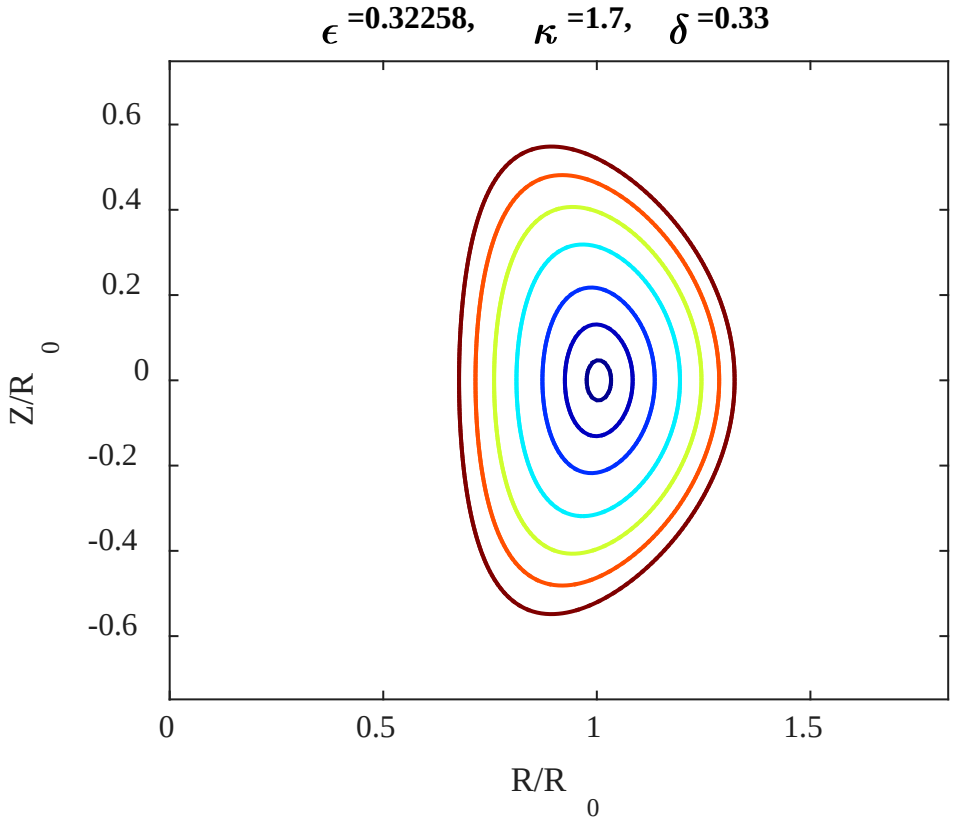

Figure 9. Magnetic flux surfaces for a force free (A=1), up-down symmetric equilibrium consistent with ITER geometrical parameters.

As expected, the flux function and hence the magnetic field are contained within a series of nested flux surfaces. For this case, $\beta = 0$ since $p = 0$ everywhere.

A very interesting effect is observed as we increase the pressure by lowering the free constant A. In the next figure, we can see the results for $A = 0$, which corresponds to the situation where the toroidal field remains constant, even within the plasma. The result is very similar, except for a light shift to the right of the flux surface. This

pattern is known as the *Shafranov shift*, and is due to the increment in pressure, which tends to "push outwards" the plasma. As this happens, the flux is compressed on the right hand side of the plasma, leading to an increase in the poloidal magnetic field and thus the magnetic confinement force, which balance the pressure.

At this point it is also interesting and not trivial to know which is the beta regime associated to this value of A. In order to perform the beta calculations, we need to specify the value of the vacuum toroidal magnetic field $B_0 = 5.3\mathrm{T}$, and of the plasma current $I_\phi = 15\mathrm{MA}$ which is expected for ITER. These yield a safety factor of 1.56 The value of beta this time is $\beta \approx 0.034$, which is in the order of magnitude of the values of beta in actual tokamak experiments.

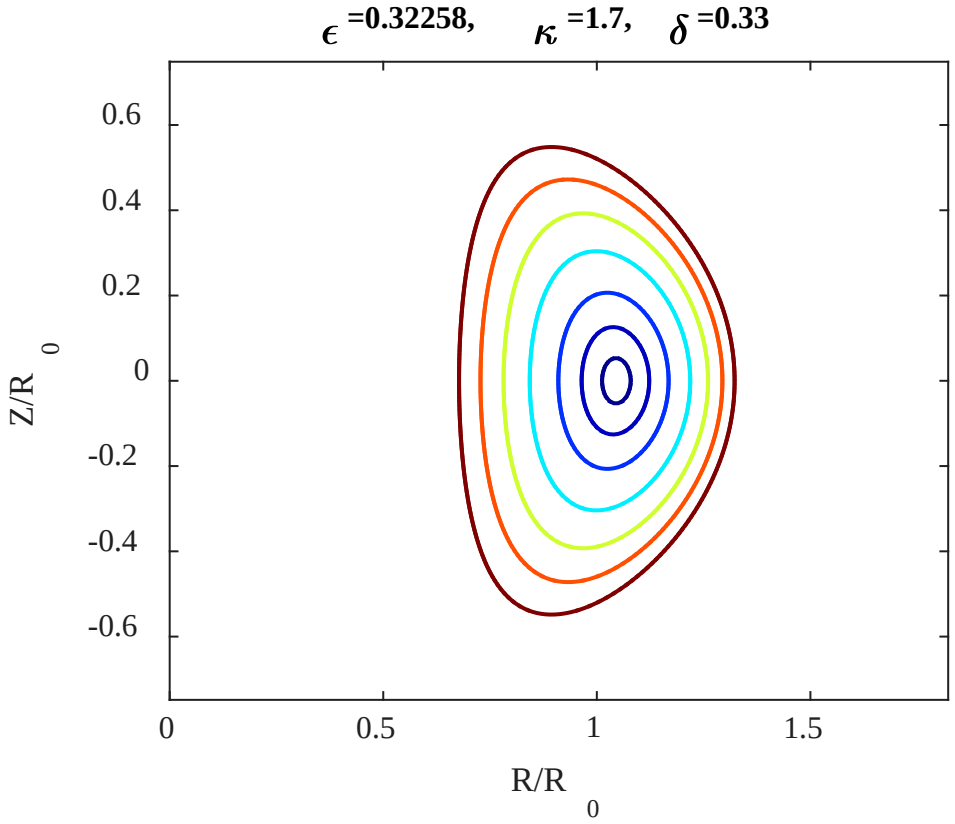

Figure 10. Flux surfaces for ITER equilibrium with A=0, i.e. constant toroidal magnetic field.

In order to compute accurately the Shafranov shift Δ, we have to define first the magnetic axis as the line that goes through the point where the flux function is a maximum or a minimum (in our case, a minimum). Due to the up-down symmetry in this case, we can set $y = 0$ and just look for the minimum for $\psi(x, 0)$. If we do so for the force free case we find that the magnetic axis is at point (0.005,0). We just have

to proceed in the same way for other values of A, or in other words, different pressures, and the difference in the position of the magnetic axis is what we mathematically define as Shafranov shift.

It is interesting to analyze the dependence of the Shafranov shift with the poloidal beta β_p. Typically, the shift is linear in β_p. We have considered for the geometrical parameters of ITER a set of different values for the free constant A, and then plotted the shift obtained in each case as a function of the poloidal beta. The result can be seen in figure 11 and it is very satisfactory. The lineal dependence is evident, although the points slightly bow down for high poloidal beta. This detail is actually observed in the literature [12].

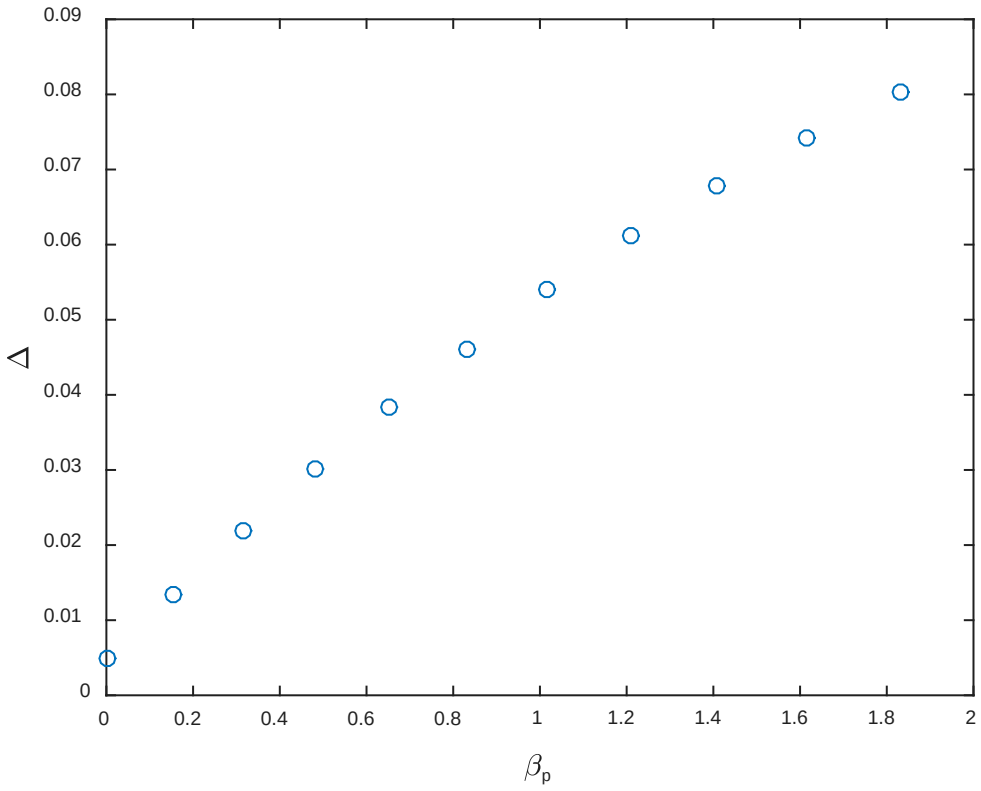

Figure 11. Shafranov shift vs poloidal beta. The lineal dependence is consistent with other papers (see Ref. 11).

We have successfully obtained the flux surfaces and some important physical parameters for a typical tokamak geometry by applying solely the ideal MHD equations and assuming that the equilibrium state can be described with Solov'ev profiles. The results are physically reasonable and in good agreement with our expectations.

Now, we can apply our algorithm to a different set of geometrical parameters, and a different toroidal magnetic field and plasma current. More specifically, we are going to study Solov'ev equilibria for the ASDEX Upgrade (AUG) tokamak located in Garching, Germany. This is the second biggest tokamak in operation in Europe and, as we previously discussed, it was in AUG where the H-mode was first achieved.

The toroidal magnetic field in AUG can reach 3.9 T, and it has a plasma current of up to 2 MA. The geometrical parameters are not completely fixed, i.e. one can generate plasmas with slightly different shapes. We are going to exploit this to see how the plasma shape and its associated physical quantities change with respect to these parameters.

We are going to start by fixing the inverse aspect ratio $\varepsilon = 0.5/1.65$, and the elongation $\kappa = 1.6$, while varying the triangularity δ. For a given A, the magnetic surfaces obtained are given in figure 12. One can realize how the plasma shape is more elliptical for small values of δ, and it becomes more triangular (hence its name) for high δ. The beta regime, however, is almost the same in both cases.

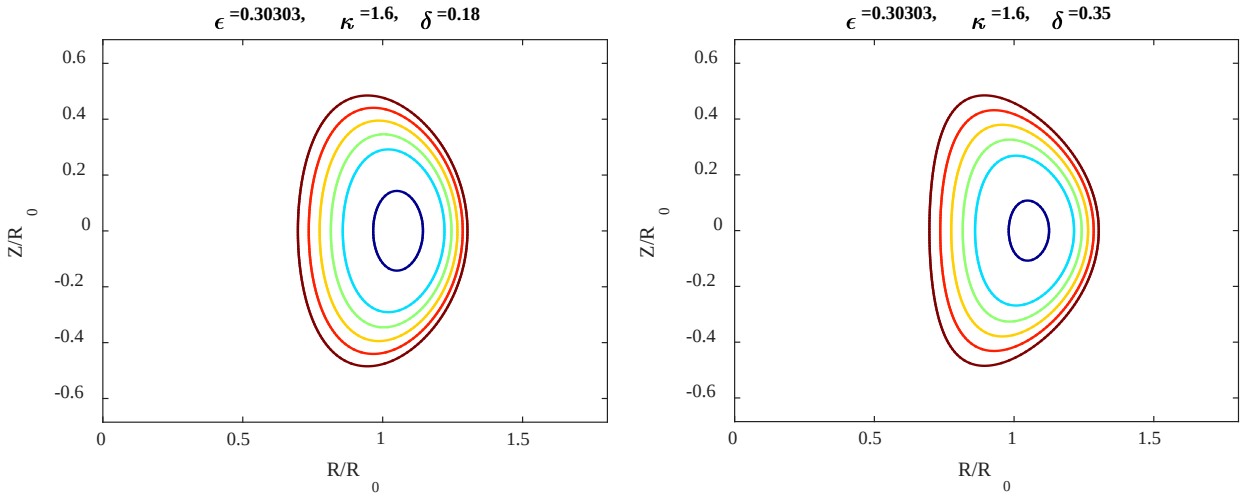

Figure 12. Flux surfaces for up-down symmetric equilibria with geometrical parameters consistent with AUG experiments, and in particular (a) minimal triangularity and (b) maximum triangularity.

Next, we set the triangularity at $\delta = 0.3$ and study the dependence of beta and the Shafranov shift with the minor radius a. In other words, we will vary the inverse aspect ratio ε and study how β and Δ change. The resulting flux surfaces are shown in figure 13.

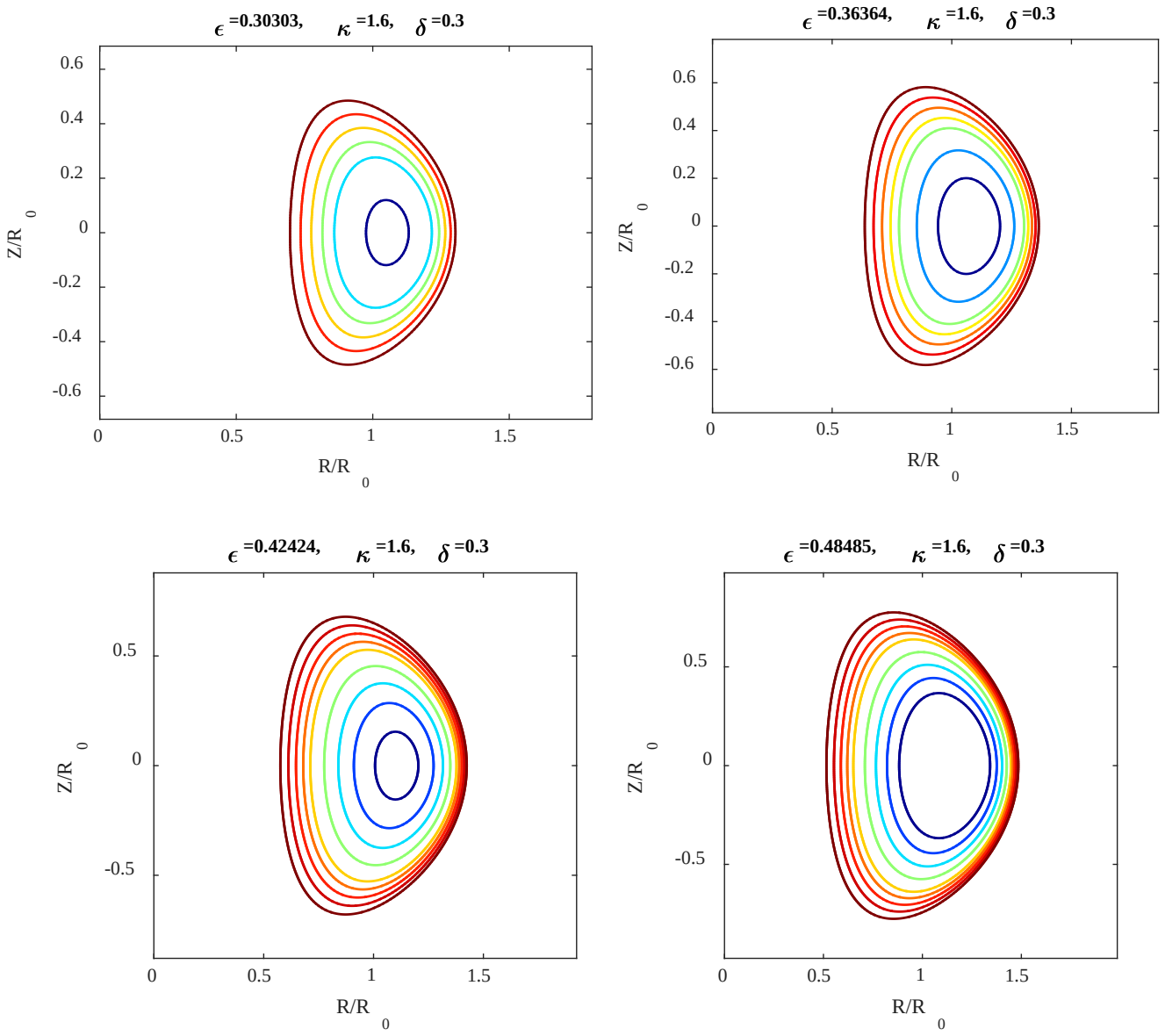

Figure 13. Flux surfaces for different values of the inverse aspect ratio ε (ϵ in the figures), all of them consistent with actual AUG plasmas.

Table 2. Normalized pressure β and Shafranov shift Δ for different values of the minor radius a.

	$a = 0.5\text{m}$	$a = 0.6\text{m}$	$a = 0.7\text{m}$	$a = 0.8\text{m}$
β	0.032	0.0252	0.0201	0.0164
Δ	0.0574	0.0826	0.1110	0.1421

Table 2 shows that for the constant value of $A = -0.5$ the total beta decreases as we increase ε, and the Shafranov shift strongly increases, following both magnitudes a linear dependence with the inverse aspect ratio.

We can also calculate the toroidal component of the magnetic field, which we expect to decrease as 1/R, as it happens in actual tokamak experiments. For this purpose, we choose for example $\varepsilon = 0.6$, and using (36), we easily obtained the magnetic field. As shown in figures 14 and 15 (below) the overall 1/R behavior is clear.

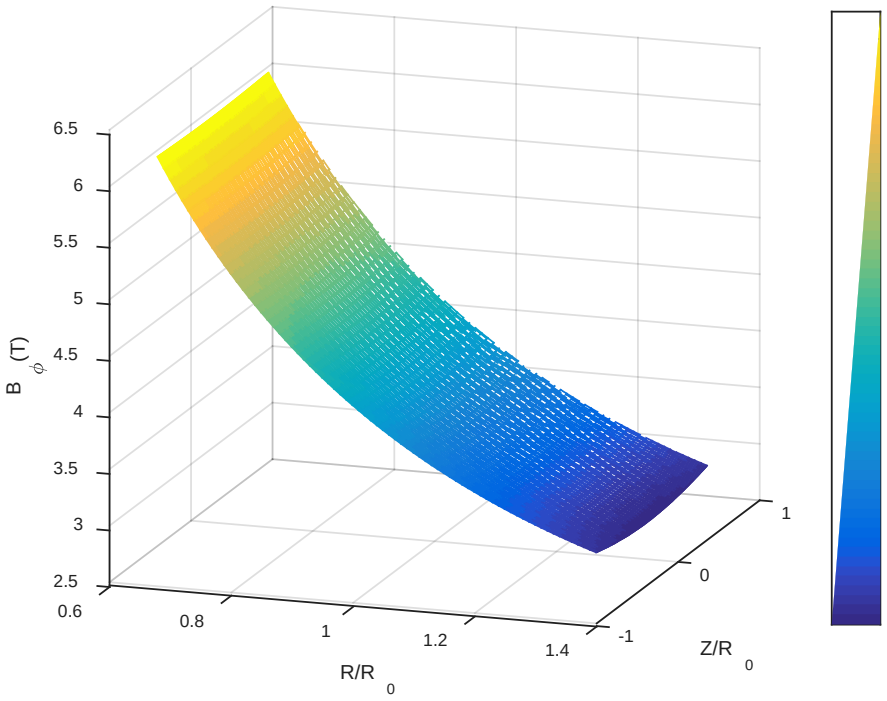

Figure 14. Toroidal magnetic field strength in the region of interest.

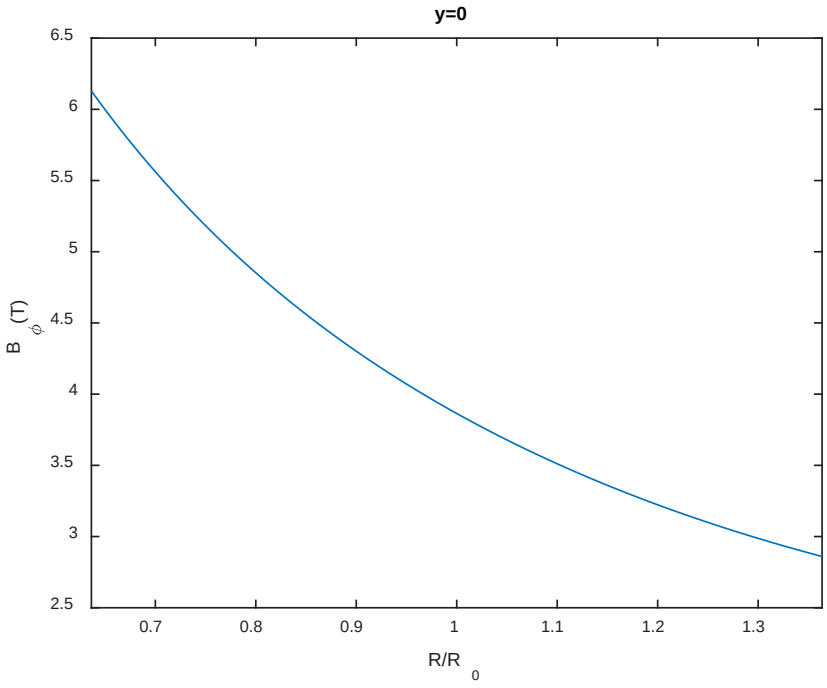

Figure 15. Toroidal magnetic field in the y=0 plane.

Even if we obtained reasonably accurate results for both ITER and AUG, the fact that we are using an up-down symmetric plasma shape is very unrealistic. Both tokamak experiments are divertor tokamaks, i.e. they generate (or will generate, in the case of ITER) up-down asymmetric plasmas with an X-point. As an example to illustrate the magnetic surfaces for this case, we can solve the GS equation for typical parameters of the NSTX (National Spherical Tokamak eXperiment), located in Princeton, USA.

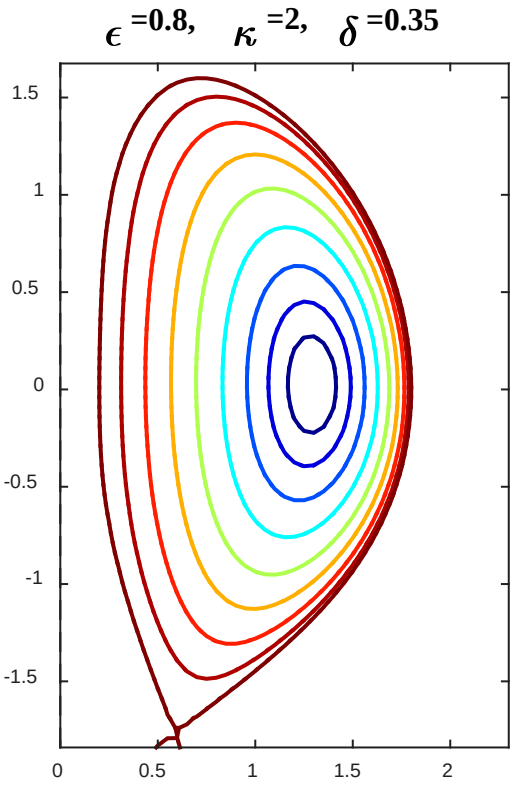

Figure 16. Magnetic flux surfaces for geometrical parameters consistent with the spherical tokamak NSTX.

The X-point is defined as the point in space where the poloidal component of the magnetic field is zero. In figure (16), it can be easily spotted at the bottom of the image. The qualitative idea behind the introduction of an X-point is to drive particles lost by the plasma to the divertor, which is located under the plasma, and it is specially design to withstand large heat fluxes, as we discussed in the introduction. Thanks to this mechanism the first wall of the tokamak receives a smaller heat flux and the damage done to it is reduced.

5.3 Taylor states: Theory

The second method we will use to find the magnetic surfaces in an axisymmetric system will study reference [13]. In this case, we will consider the flux functions corresponding to Taylor states. A plasma is said to be in a Taylor state when the following relation is fulfilled by the magnetic field in the plasma [14]

$$\nabla \times \boldsymbol{B} = \lambda \boldsymbol{B}, \tag{41}$$

where λ is a constant.

Plasmas tend to relax to these states because they minimize their magnetic energy. A great advantage of this method is that one does not need to introduce by hand the form of the pressure and the toroidal magnetic field like we did for the Solov'ev equilibrium. It is also worth to mention that this relation is not only valid for fusion plasmas, but also for astrophysical plasmas. From this condition, we can derive its associated GS equation and solve for the flux function using the adequate boundary conditions, just as was done in 5.2. The derivation of the equation for ψ is somewhat similar to the GS one from the ideal MHD.

First, we write the current density in terms of the flux function

$$\mu_0 \boldsymbol{J} = -\frac{1}{R}\Delta^* \psi \, \boldsymbol{e_\phi} + \frac{1}{R}\nabla F(\psi) \times \boldsymbol{e_\phi}. \tag{42}$$

The first term on the right hand side is of course the toroidal component of the current, and the second term is a compact way of writing the poloidal component.
We can also write the magnetic field in terms of its toroidal and poloidal components

$$\boldsymbol{B} = \frac{F(\psi)}{R}\boldsymbol{e_\phi} + \frac{1}{R}\nabla\psi \times \boldsymbol{e_\phi}. \tag{43}$$

Now since equation (41) implies $\lambda \boldsymbol{B} = \mu_0 \boldsymbol{J}$, we can use these who equations to obtain a relation for the toroidal component, and another one for the poloidal component

$$-\Delta^* \psi = \lambda \, F(\psi), \qquad \frac{dF}{d\psi} = \lambda. \tag{44}$$

If we set $\psi = 0$ on the plasma boundary, we can directly integrate the poloidal component equation. In order to ease the calculations, we will set the integration constant F_0 to zero, which means that the toroidal component at the plasma edge is assumed to be zero. This is an adequate choice for spheromak plasmas, since they have no vacuum toroidal field. Substituting $F(\psi) = \lambda\psi$ in the toroidal component equation we get

$$\Delta^*\psi = -\lambda^2\psi. \tag{45}$$

This is a well-known Helmholtz problem that can be solved by separation of variables. The solution of this eigenvalue problem has an infinite number of terms, from which we will take a linear combination of the following eleven functions as an approximate solution

$$\begin{aligned}\psi = \psi_0 + c_1\psi_1 + c_2\psi_2 + c_3\psi_3 + c_4\psi_4 + c_5\psi_5 + c_6\psi_6 + c_7\psi_7 + c_8\psi_8 \\ + c_9\psi_9 + c_{10}\psi_{10}\end{aligned} \tag{46}$$

$$\begin{gathered}\psi_0 = RJ_1(c_{12}R) \quad \psi_1 = R\,Y_1(c_{12}R) \quad \psi_2 = RJ_1\left(\sqrt{{c_{12}}^2 - {c_{11}}^2}R\right)\cos(c_{11}Z) \\ \psi_3 = R\,Y_1\left(\sqrt{{c_{12}}^2 - {c_{11}}^2}R\right)\cos(c_{11}Z) \qquad \psi_4 = \cos\left(c_{12}\sqrt{R^2 + Z^2}\right)\end{gathered}$$

$$\begin{gathered}\psi_5 = \cos(c_{12}Z) \qquad \psi_6 = RJ_1(c_{12}R)Z \qquad \psi_7 = R\,Y_1(c_{12}R)Z \\ \psi_8 = R\,Y_1\left(\sqrt{{c_{12}}^2 - {c_{11}}^2}R\right)\sin(c_{11}Z)\end{gathered} \tag{47}$$

$$\psi_9 = R\,Y_1\left(\sqrt{{c_{12}}^2 - {c_{11}}^2}R\right)\sin(c_{11}Z) \qquad \psi_{10} = \cos(c_{12}Z).$$

Where J_1 and Y_1 are the first order Bessel functions of the first and second kind, respectively, $c_{12} = \lambda$, and $c_{11} = k$ is the separation constant that appears in the separation of variables procedure. Now we need to consider 12 boundary conditions to close the problem.

We will consider again that the plasma boundary can be parametrized through (30), and the boundary conditions will be imposed as in the previous method, by ensuring $\psi = 0$ on the border and that the curvature is smooth through equations (31). Furthermore, since we are aiming for up-down asymmetric equilibria, we need to include the constraints that make the poloidal field zero at the X-point with coordinates (R_X, Z_X)

$$\psi(R_X, Z_X) = 0 \qquad \frac{\partial\psi}{\partial R}(R_X, Z_X) = 0 \qquad \frac{\partial\psi}{\partial Z}(R_X, Z_X) = 0, \tag{48}$$

and the conditions that give the slope of the plasma boundary at the inner equatorial point and outer equatorial point (see figure 8), which are necessary due to the lack of up-down symmetry

$$\frac{\partial \psi}{\partial Z}(1+\varepsilon, 0) = 0 \qquad \frac{\partial \psi}{\partial Z}(1-\varepsilon, 0) = 0. \tag{49}$$

Putting together all the boundary conditions, we end up with a non-linear system of 12 equations that can be solved with MATLAB.

5.4 Taylor states: Results

We can finally then compute the flux surfaces for a given set of geometrical parameters and location of the X-point. As an example, we will take $\varepsilon = 0.9$, $\kappa = 1.15$ and $\delta = 0$, and the X-point located at $(1 + 0.5\varepsilon, 1.25\varepsilon\kappa)$. The resolution for the flux function obtained in this case is illustrated in figure (17).

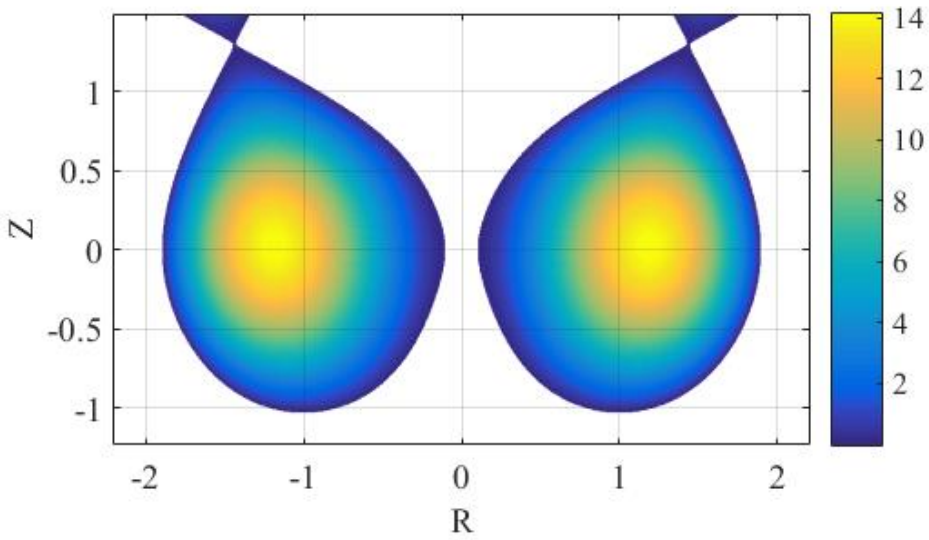

Figure 17. Flux function plot for typical spheromak geometric parameters. Note that, in the case of spheromaks, the inverse aspect ratio and the elongation are near to the unity, and the triangularity is very small. These conditions give the plasma its characteristic spherical shape.

6. Conclusions

In summary, a fairly detailed overview of the current state of fusion research has been given. Also, we have introduced the basic aspects of the fusion reactions that will take place in future commercial reactors. More importantly, we have introduced the problem of equilibrium of plasmas, that must be well-known in order to develop a competitive fusion power plant in the future. In particular, we looked at two different methods.

First, we considered the ideal MHD model and its related equilibrium, which took us to the Grad-Shafranov equation. Even if this is a very old, simple model to describe plasmas, the GS equation is extremely complicated and it is still today a field of research. As an example of this, we presented one moderately recent procedure to find solutions to the GS equation based on Solov'ev equilibrium. We also wrote some additional code to calculate a variety of physical quantities of interest that can be obtained with the solutions to GS and some additional experimental parameters, such as the vacuum toroidal magnetic field. In particular, we presented the calculations of the beta regime, the Shafranov shift and the toroidal magnetic field profile for a given GS solution. All of them agreed very well with the expected results.
Second, for the sake of completion, we consider the application of the more recently developed Taylor states. We only considered its application to spheromak plasmas, due to the fact that the calculations are simpler than for other fusion plasmas.

In conclusion, we have investigated in detail the equilibrium problem in fusion plasma physics, which is crucial for plasma confinement in a future fusion power plant.

7. Acknowledgements

There are a few people that have contributed essentially to the development of this work. First, I want to express my gratitude to my family for patiently listening to most of the content here presented. Second, I want to thank my colleague José Manuel for teaching me to calculate surface integrals on a non-trivial region in MATLAB. Third and last, I want to thank my tutor José Cotrino for his great readiness to help me in this work and for the huge amount of reading provided about this subject.

8. Bibliography

[1] J. Ongena, R. Koch, R. Wolf, and H. Zohm, “Magnetic-confinement fusion,” *Nat. Phys.*, vol. 12, no. May, pp. 398–410, 2016.

[2] D. . Campbell, “The first fusion reactor: ITER,” *Europhys. news*, vol. 47, no. 5&6, p. 52, 2016.

[3] F. Wagner, “The history of research into improved confinement regimes,” *Eur. Phys. J. H*, pp. 1–27, 2017.

[4] F. Wagner *et al.*, “Regime of Improved Confinement and High Beta in Neutral-Beam-Heated Divertor Discharges of the ASDEX Tokamak,” *Phys. Rev. Lett.*, vol. 49, no. 19, pp. 1408–1412, Nov. 1982.

[5] H. S. Xie, Y. Xiao, and Z. Lin, “A New Paradigm for Turbulent Transport Across a Steep Gradient in Toroidal Plasmas,” *Phys. Rev. Lett.*, vol. 118, no. March, pp. 20–22, 2017.

[6] K. . Nishikawa and M. Wakatani, *Plasma Physics - Basic Theory with Fusion Applications*, vol. 1–2. 2015.

[7] J. P. Freidberg, *Plasma physics and fusion energy*, vol. 1. 2007.

[8] A. C. C. Sips, “Advanced scenarios for ITER operation,” *Plasma Phys. Control. Fusion*, vol. 47, no. 5A, pp. A19–A40, 2004.

[9] T. J. M. Boyd and J. J. Sanderson, *The Physics of Plasmas*. Cambridge University Press, 2003.

[10] A. J. Cerfon and J. P. Freidberg, “‘one size fits all’ analytic solutions to the Grad-Shafranov equation,” *Phys. Plasmas*, vol. 17, no. 3, 2010.

[11] S. B. Zheng, A. J. Wootton, and E. R. Solano, “Analytical tokamak equilibrium for shaped plasmas,” *Phys. Plasmas*, vol. 3, no. 3, pp. 1176–1178, 1996.

[12] J. Choi, H. Choi, and O. Kwon, “Dependence of the Shafranov Shift in Tokamaks on the Plasma Parameters,” *New Phys. Sae Mulli*, vol. 65, no. 3, pp. 297–301, 2015.

[13] A. J. Cerfon and M. O’Neil, “Exact axisymmetric Taylor states for shaped plasmas,” *Phys. Plasmas*, vol. 21, no. 6, pp. 1–5, 2014.

[14] J. B. Taylor, “Relaxation and magnetic reconnection in plasmas,” *Rev. Mod. Phys.*, vol. 58, no. 3, pp. 741–763, 1986.